Binding Analysis of 1α- and 17α-Dihydrotestosterone Derivatives to Homodimeric Sex Hormone-Binding Globulin

Jochen Metzger,[‡] Andreas Schnitzbauer,[‡] Manuela Meyer,[‡] Monika Söder,[‡] Claude Y. Cuilleron,[§] Hagen Hauptmann,[||] Erasmus Huber,[⊥] and Peter B. Luppa*[,‡]

Institute for Clinical Chemistry and Pathobiochemistry, Klinikum rechts der Isar der Technischen Universität München, Ismaninger Strasse 22, 81675 Munich, Germany, INSERM ERM 0322, Hôpital Debrousse, 29 rue Soeur Bouvier, 69322 Lyon Cedex 05, France, Institute of Organic Chemistry, Universität Regensburg, Universitätsstrasse 31, 93053 Regensburg, Germany, and Roche Diagnostics GmbH, Werk Penzberg, Nonnenwald 2, 82377 Penzberg, Germany

Received July 18, 2003; Revised Manuscript Received September 25, 2003

ABSTRACT: Binding studies of the interaction of immobilized 1α- and 17α-aminoalkyl derivatives of 5α-dihydrotestosterone (DHT) with purified *N*-deglycosylated homodimeric human sex hormone-binding globulin (SHBG) were performed using a surface plasmon resonance biosensor. These 1α- and 17α-derivatives with spacers of appropriate lengths between the amine function and the steroid ring skeleton enabled privileged, sterically undisturbed, interactions of either the 17- or 3-characteristic functional groups of DHT with SHBG. The association constants (K_a1) for the binding of these immobilized DHT derivatives to the first binding site of SHBG, determined by SPR measurements, were 0.16×10^7 M^{-1} for 17α-aminopropyl-17β-hydroxy-5α-androstan-3-one (**1**), 1.64×10^7 M^{-1} for 17α-aminocaproyl-17β-hydroxy-5α-androstan-3-one (**2**), and 1.2×10^8 M^{-1} for 1α-aminohexyl-17β-hydroxy-5α-androstan-3-one (**3**). These values were compared with global K_a data for the corresponding nonimmobilized DHT derivatives from equilibrium measurements using competitions with a tritiated testosterone tracer: the K_a values were 1.25×10^7 M^{-1} for **1**, 1.50×10^7 M^{-1} for **2**, and 140×10^7 M^{-1} for **3**, confirming a remarkably high binding affinity of this latter compound for SHBG. A global fitting analysis of the biosensor data revealed that the interaction of the three immobilized steroids with SHBG was best described by a kinetic model assuming two structurally independent binding sites. This hypothesis of a bivalent binding model was also directly suggested by a dual fluorescent signal observed by the flow cytometry analysis of SHBG immobilized as a hybrid complex binding simultaneously two 1α-aminohexyl DHT ligands, one formed by **3**, covalently coupled to phycoerythrin-labeled latex microspheres, and the other by the same DHT derivative, coupled to a fluorescein derivative (**4**).

Human sex hormone-binding globulin (SHBG),[1] a 93.4-kDa homodimeric glycoprotein produced by hepatocytes, is the major sex steroid-binding protein in plasma (*1*). SHBG binds testosterone (T), 5α-dihydrotestosterone (DHT), as well as 17β-estradiol (E2) and related steroids in plasma with high affinity (*2*−*5*). The glycoprotein is a product of a single gene located on the short arm of chromosome 17 (*6*, *7*). The glycosylation of the monomeric protein forms one *O*-linked oligosaccharide at Thr-7 and two *N*-linked oligosaccharides at Asn-351 and -367 in the C-terminal region of the molecule (*8*, *9*). The two monomers of SHBG interact very strongly with each other even in the absence of a steroid ligand (*10*), although the dimerization is promoted in the presence of ligand (*11*) and, independently, of divalent cations such as calcium or zinc (*12*).

The major physiological role of SHBG is the regulation of bioavailability of T and E2 by controlling their balance and their respective metabolic clearance rates (*13*−*16*). SHBG has also been reported to exert an influence on the uptake of sex steroids (*17*−*19*) in target cells and in signal transduction (*20*, *21*). Plasma SHBG levels vary considerably between individuals and are influenced by hormonal, metabolic, and nutritional factors (*1*). It is of clinical interest that low serum levels of SHBG have been found in women suffering from disorders characterized by androgen excess (*1*), and are also considered as a prognostic indicator for the onset of type II diabetes mellitus, hyperthyroidism, and cardiovascular disease (*22*). Thus, the understanding of the interaction between steroid ligands and SHBG, the measure-

* To whom correspondence should be addressed. Fax +49 89 4140 4875; e-mail luppa@klinchem.med.tum.de.

‡ Klinikum rechts der Isar der Technischen Universität München.

§ INSERM ERM 0322, Hôpital Debrousse.

|| Universität Regensburg.

⊥ Roche Diagnostics GmbH.

[1] Abbreviations: AEC, 3-amino-9-ethylcarbazole; BSA, bovine serum albumin; CM, carboxymethyl; DMF, dimethyl formamide; DMSO, dimethyl sulfoxide; DHT, 5α-dihydrotestosterone; E2, 17β-estradiol; EDC, *N*-ethyl-*N*′-(3-diethylaminopropyl)-carbodiimide; FC, flow cell; FL, fluorescence channel; FITC, fluorescein isothiocyanate; FLUOS, 5-carboxy-fluorescein *N*-hydroxysuccinimidyl ester; FSC, forward scatter; HBS, HEPES-buffered saline; HEPES, *N*-(2-hydroxyethyl)-piperazine-*N*′-(2-ethanesulfonic acid); HRP, horseradish peroxidase; LBD, ligand-binding domain; mAb, monoclonal antibody; MES, 2-[*N*-morpholino]-ethanesulfonic acid; MFI, mean fluorescence intensity; NHS, *N*-hydroxysuccinimide; pAb, polyclonal antibody; PBS, phosphate-buffered saline; PE, R-phycoerythrin; PNGase F, peptide *N*-glycosidase F; PVDF, polyvinylidenfluoride; RBA, relative binding activity; RI, refractive index; RU, resonance unit; SD, standard deviation; SDS−PAGE, sodium dodecyl sulfate−polyacrylamide gel electrophoresis; SHBG, sex hormone-binding globulin; SPR, surface plasmon resonance; SSC, side scatter; T, testosterone.

10.1021/bi035269k CCC: $25.00
Published on Web 10/31/2003

ment of protein-bound and free steroid fractions (*23*), and the knowledge of factors regulating SHBG levels, are of great endocrinological significance.

Optimal steroid binding to SHBG requires a planar C_{19} steroid with a 17β-hydroxyl group and an electronegative functional group at C-3 (*24*). The recently reported crystal structure of the *N*-terminal recombinant human SHBG ligand-binding domain (LBD) complexed with steroidal ligands (*25*) has revealed a homodimeric structure in which each recombinant monomer contains a LBD for a steroid molecule, intercalated into the hydrophobic core. Additionally, recent site-directed mutagenesis experiments have shown that dimerization-deficient SHBG variants still contain a LBD with an affinity and specificity indistinguishable from wild-type SHBG (*25*, *26*). Until these observations were reported, the commonly accepted hypothesis of an equimolar relationship between homodimeric SHBG and steroidal ligand has seldomly been questioned (*27*). According to the crystallographic data, the oxygen atom at C-3 of ring A of DHT is anchored in the interior of the protein, while rings A and B are completely buried. Most of the structural modifications of the steroid ligand significantly reduce the relative binding affinities for SHBG (*3*) except for substitutions at positions C-4, C-12α, and C-17 which are well tolerated (*28*−*30*). Mesterolone (17β-hydroxy-1α-methyl-5α-androstan-3-one) also shows a high affinity for human SHBG (*29*). This suggests that the 1α position might be qualified as a potential candidate for introducing a larger substituent to produce novel efficient SHBG ligands, structurally complementary to the known 17α-DHT ligands (*31*) since the D-ring instead of A-ring becomes optimally exposed for interacting with SHBG. However, according to the shape of the SHBG binding site, we speculated that a long hydrophobic 1α-alkyl chain could have a reasonable probability to be accommodated without too much sterical clashes with proximal amino acids on the β-side of the 1-position.

In a preliminary study, we could demonstrate that the introduction of an unsubstituted 1α-aminohexyl linkage on the A-ring of DHT leads to a higher binding affinity for human SHBG than unsubstituted 17α-aminoalkyl DHT derivatives (*31*). This finding prompted us to collect further physicochemical data on the biochemical interaction of these two families of androgen ligands with SHBG in the view of determining whether a mechanism involving the two potential steroid binding sites of native SHBG could be detected. The 1α- and 17α-aminoalkyl DHT derivatives, substituted at the two opposite A- and D-ring extremities of the steroid skeleton, were covalently coupled onto commercially available carboxymethylated (CM) dextran coated biosensor chips designed for surface plasmon resonance (SPR) technology, thus allowing kinetic studies aimed at analyzing the binding mechanisms of these immobilized steroids with native soluble human SHBG. The reactive amine function of the 1α- and 17α-DHT derivatives additionally offered the possibility of coupling these compounds to latex microspheres. Thus, flow cytometry could also be employed as an independent method for evaluating whether the homodimeric SHBG, already bound to a steroid immobilized on fluorescent latex beads has still a second LBD available for binding a second soluble steroid ligand coupled to another fluorescent molecule.

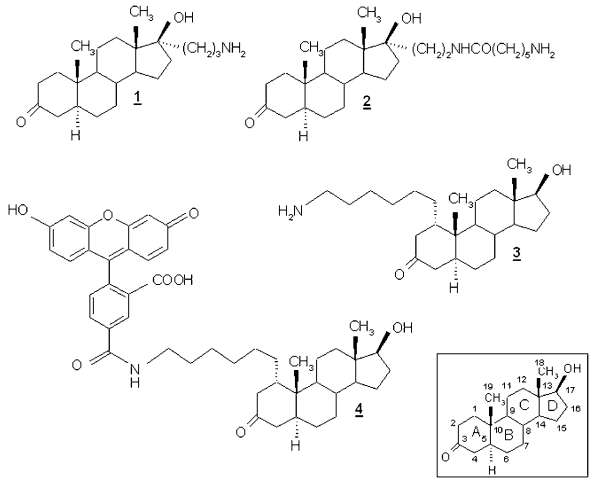

FIGURE 1: Steroidal DHT derivatives **1**−**4** used for the study. In the inset numbering and ring letters of DHT are given according to the IUPAC recommendations from 1989.

EXPERIMENTAL PROCEDURES

Chemicals. F1- and B1-chips (research grade), as well as *N*-hydroxysuccinimide (NHS), *N*-ethyl-*N*′-(3-diethyl-aminopropyl)-carbodiimide (EDC), ethanolamine-HCl, and HEPES-buffered saline (HBS) (10 mM HEPES with 0.15 M NaCl, 3.4 mM EDTA and 0.005% surfactant P20 at pH 7.4) were purchased in the original format from Biacore. Con A-Sepharose was from Amersham Pharmacia Biotech, Freiburg, Germany, and peptide *N*-glycosidase F (PNGase F, 500 000 U/mL) from New England BioLabs, Beverly, MA. 5α-Dihydrotestosterone (DHT, 17β-hydroxy-5α-androstan-3-one) and testosterone (T, 17β-hydroxy-4-androsten-3-one) were from Merck, Darmstadt, Germany, [1,2,6,7-^{3}H]-T (specific activity: 2.92 TBq/mmol) was from Amersham Pharmacia Biotech. 5-Carboxyfluorescein *N*-hydroxysuccinimidyl ester (FLUOS) was from Molecular Probes, Eugene, OR. The COOH-activated, streptavidin-conjugated latex beads (1% s/v in 10 mM phosphate-buffered saline (PBS); 1.01 μm average diameter, SD 2.5%) were from Sigma, Deisenhofen, Germany, whereas biotin-R-phycoerythrin (Biotin-PE, stock solution 1 mg/mL in 50 mM sodium phosphate buffer, pH 7.0) was purchased from DPC Biermann, Bad Nauheim, Germany. All other laboratory chemicals, including 3-amino-9-ethylcarbazole (AEC), were from Sigma.

Antibodies. The monoclonal anti-testosterone antibodies (mAbs) E2−3 (clone M40557), T-19 (clone M212051a), and T-3 (clone M211244) were from Fitzgerald Industries (Concord, MA). The polyclonal rabbit anti-SHBG antibody (pAb) was from Dako A/S, Glostrup, Denmark. Fluorescein isothiocyanate (FITC)-conjugated goat anti-rabbit IgG pAb was purchased from Dianova, Hamburg, Germany, whereas a secondary horseradish peroxidase (HRP)-conjugated donkey anti-rabbit IgG pAb was from Amersham Pharmacia Biotech.

Synthesis. The chemical syntheses of the 1α- and 17α-DHT derivatives (**1**−**3**) (Figure 1) have been previously reported (*31*)**.**

The synthesis of 1α-(5′-carboxyfluorescein-*N*-amidohexyl)-17βhydroxy-5α-androstan-3-one (**4**) was performed as follows: 0.9 mg (2.14 μmol) of **1** (as hydrochloride) was dissolved in 0.5 mL of freshly distilled dimethyl formamide (DMF). Subsequently, a solution of 1.5 mg (3.17 μmol) of

5-carboxyfluorescein *N*-hydroxysuccinimide ester (FLUOS) in 0.5 mL of DMF along with 0.6 μL of triethylamine was added. The reaction vessel was sealed and stirred under an argon atmosphere. After 2 h the pH was adjusted to 8.0 by further addition of triethylamine. The solution was kept under argon overnight, and then the solvent was evaporated. The product **4** was dissolved in 160 μL of DMF and purified by semipreparative HPLC on a Vydac C_{18} column (4.6 × 250 mm, 300 Å, 5 μm; flow 1 mL/min) using the following elution gradient: $t = 0$ min, 100% A, 0% B; $t = 20$ min, 5% A, 95% B. Eluent A: H_2O/0.1% trifluoroacetic acid, eluent B: acetonitrile/0.1% trifluoroacetic acid. The major product was eluted at 72% B in a single peak. This peak was collected in several fractions, which were pooled after testing purity by analytical HPLC using the same solvent system as mentioned above. The structure was confirmed by mass spectrometry using a Q-TOF 2 apparatus (ion source: Z-Spray) from Micromass, Manchester, UK. MS (ESI, *m*/*z*, relative intensity %): 748.35 ($M+H^+$ 100%).

*Particle Preparation and Coupling of Compound **3** to Carboxylate-Activated Latex Beads.* For the flow cytometry experiments the 1α-aminohexyl-DHT derivative **3** was coupled via EDC/NHS-chemistry to the COOH-activated, streptavidin-conjugated latex beads. One microliter of the latex bead suspension was washed twice in 1 mL of PBS. After a final centrifugation for 5 min at 10000*g*, the supernatant was removed and the beads were incubated for 30 min with 20 μg of Biotin-PE. Subsequently, the PE-labeled beads were washed with 0.5 M 2-[*N*-morpholino]-ethanesulfonic acid (MES), containing 25 mg/mL $NaHCO_3$ (pH 6.8), and activated with 50 μL of 400 mM EDC in bidistilled H_2O for 20 min at room temperature. Then 50 μL of 100 mM NHS in bidistilled H_2O was added and the incubation was continued for a further 20 min. The suspension was centrifuged at 10000*g* and the beads were washed twice with MES buffer. For the steroid coupling, 300 μL of a solution containing 130 μM 1α-aminohexyl DHT **3** and 130 μM ethanolamine in 0.1 M MES plus 5 mg/mL $NaHCO_3$ were added. Following a 1-h incubation with two subsequent washing steps, unreacted active ester groups on the bead surface were blocked by incubation with 200 μL of a 1 M ethanolamine solution in MES buffer for 10 min.

Preparation of N-Deglycosylated Homodimeric SHBG. We used SHBG affinity purified from human pregnancy plasma (>98% by SDS−PAGE, lot no. A0011105) purchased from Fitzgerald Industries International, Concord, MA. A total of 100 μL of a concentrated SHBG solution (5 mg/mL) were prepared in bidistilled H_2O from the supplied lyophilized material (initially dissolved in 0.1 M PBS, pH 7.4, with 0.2% NaN_3). Five units PNGase F per μg of SHBG were added and a 30-min incubation at 37 °C was performed. Subsequently, the analytical size-exclusion chromatography was performed according to a protocol given in ref *31*. The pooled fractions of the main peak (at 64.56 min) were concentrated using Microcon centrifugal filters (Millipore, Schwalbach, Germany) with a molecular weight cutoff of 30 kDa. After adjustment to a protein concentration of 0.2 mg/mL (2.2 μM), the *N*-deglycosylated homodimeric SHBG was stored in aliquots at −20 °C until biosensor and flow cytometry measurements.

Measurement of Immunoreactive SHBG and Free T in Serum. SHBG was measured in serum samples with the ^{125}I-labeled SHBG IRMA kit from Orion (Espoo, Finland). For the determination of free T levels the ^{125}I-labeled direct free T Coat-A-Count RIA from DPC−Biermann, Bad Nauheim, Germany, was used. For γ-counting we used a 1277 Gamma master counter from LKB Wallac, Bromma, Sweden.

Equilibrium Measurements. Relative binding activities (RBA) of the 1α- and 17α-DHT derivatives **1**, **2**, and **3** were determined under equilibrium conditions at 37 °C using ^{3}H−T as tracer, and Con A-Sepharose as solid separation phase, as described in detail in ref *31*.

SPR Biosensor Measurements. The kinetic ligand-binding measurements were performed on the BIAcore X system (Biacore AB, Uppsala, Sweden) using Pioneer B1-chips. Generally, the interaction of proteins/receptors with their respective ligands, immobilized on the sensor chip, is monitored as a function of time (as SPR sensorgrams), expressed in arbitrary resonance units (RU). One RU represents a change of 0.0001° in the angle of the intensity minimum. For most proteins (including SHBG), this is roughly equivalent to a change in concentration of about 1 pg/mm^2 on the sensor surface.

The 17α- and 1α-aminoalkyl DHT derivatives (**1**−**3**) were immobilized onto B1-chips via the NHS/EDC method using the original Biacore amine coupling kit according to the manufacturer's instructions: while maintaining a continuous flow of 5 μL/min HBS-P buffer over the sensor surface at 25 °C, the carboxyl groups of the dextran layer were activated with an injection of a 1:1-solution of 0.2 M EDC and 0.05 M NHS for 7 min followed by a further manual 6-min injection of a mixture of 100 μM aminoalkyl DHT derivative and 200 μM of ethanolamine in 100 mM borate buffer (pH 9.0) to ensure a low steroid surface density (*32*). After the signal reached approximately 200−350 RU, the unreacted active ester groups were blocked by a 7-min injection of a 1.0 M ethanolamine hydrochloride solution. In general, the flow cell FC2 of the BIAcore X instrument was used for coating the steroidal ligands, whereas the reference cell FC1 was used for a similar coating in the absence of steroid/ethanolamine so as to allow the subtraction of nonspecific binding phenomena. The binding functionality of the steroid-coated B1-surface was tested with two different anti-T mAbs, both highly cross-reactive with DHT. The mAbs were applied at a concentration of 40 μg/mL (final) in a volume of 30 μL. The *N*-deglycosylated SHBG solutions were applied in various concentrations (50−250 nM final for the 17α-DHT compounds **1** and **2**; 75−400 nM final for the 1α-DHT compound **3**, in a volume of 75 μL each). For the ligand-binding measurements a temperature of 25 °C and flow rates of 10 μL/min were chosen. The total sensorgram recording times were 1050 s (delay time 600 s). In a typical run, SHBG was injected into the flow cell over the solid-state surface. This period defined the association phase, after that the switch to buffer injection started the dissociation phase. At the end of the delay time, after the dissociation phase, an acidic buffer (100 mM H_3PO_4) was added for regenerating the chip surface.

Analysis of Kinetic Data. Association and dissociation data were calculated by the BiaEvaluation program (Biacore, version 3.0.1.). The evaluation algorithms perform a non-linear regression analysis of the measured sensorgrams. Binding events can follow the respective interaction models: 1:1 binding; 1:1 binding with mass transfer; bivalent

analyte binding; heterogeneous analyte or ligand binding and two-state reaction with conformational change. The most appropriate model was chosen by a fitting analysis based on the residual plots with low χ^2 values which were obtained from analysis of the sensorgrams, the χ^2 value being a standard statistical measure of the closeness of fit.

Flow Cytometry Analysis. The fluorescent latex beads, covalently coupled to the 1α-aminohexyl DHT derivative **3**, were incubated for 90 min with 10 μg of PNGase F-digested, gel-purified SHBG in PBS/0.02% Tween-20 at room temperature. After two washing cycles, latex beads were stained with 0.2 μg of the HPLC-purified FLUOS derivative **4** (from a stock solution at 2 mg/mL in DMSO) in PBS/0.02% Tween-20 for 60 min at room temperature. In parallel, preparations of **4** mixed with a 10-fold molar excess of unlabeled **2** or **3**, respectively, were used for competition analysis. The latex beads were washed twice, resuspended in 1 mL of PBS, and directly used for cytometric measurements. The density of SHBG, bound on the latex bead surface, was evaluated with an immunofluorescence method using a SHBG-specific primary and a FITC-labeled secondary antibody preparation. In brief, after exposure to SHBG, beads were stained with a 4.7 mg/mL solution of rabbit anti-SHBG pAb for 60 min and a 1.5 mg/mL solution of FITC-labeled goat anti-rabbit pAb for 20 min in PBS supplemented with 1% BSA at room temperature. A preparation of fluorescent latex beads covalently coupled to the 1α-aminohexyl DHT derivative **3**, not exposed to SHBG, served as control to exclude nonspecific binding of the antibodies.

An Epics Elite ESP flow cytometer (Beckman Coulter, Hialeah, FL) was used to interrogate microspheric beads. The excitation wavelength of the laser was 488 nm. The approriate optical filters were 525 nm for the FLUOS (FL1 channel) and 575 nm for the PE fluorochrome (FL2 channel). Forward (FSC) and side (SSC) scatter properties were used to exclude aggregates formed by the COOH-activated, streptavidin-conjugated latex beads. Each fluoresence analysis was performed on the basis of a total number of 25 000 gated events. Beads labeled with either FLUOS/fluorescein or PE alone were used to find the best compensation settings for all subsequently performed two color analyses. For data evaluation and presentation the WinMDI software, version 2.8, by Joe Trotter (Scripps Research Institute, La Jolla, CA) was used.

RESULTS

Purification and Characterization of SHBG. Digestion and Purification. We used commercially available human SHBG, affinity purified from pooled pregnancy sera. Although the purity of this SHBG was high (>98% by SDS−PAGE), a deglycosylation of *N*-linked carbohydrates was performed with PNGase F to improve the homogeneity of the SHBG preparation used for the experiments, and was followed by a stringent size-exclusion chromatography procedure to lower possible contamination by both oligomeric forms of SHBG and bound steroidal ligands (*33*). Native SHBG and PNGase F digested SHBG both after size-exclusion chromatography were controlled by an immunoblot after SDS−PAGE (Figure 2). For native SHBG (lane 1) the presence of two distinct bands at molecular masses of approximately 50 and 47 kDa

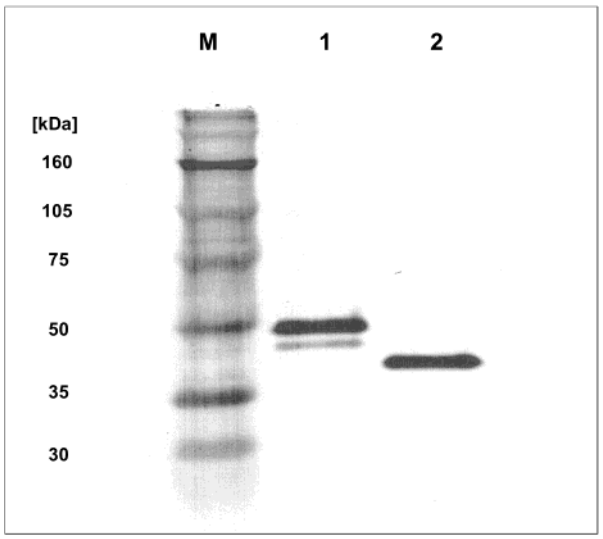

FIGURE 2: Immunoblotting of processed SHBG after separation in a 10% SDS−polyacrylamide gel. SHBG gel filtration preparation before (1) and after PNGase F digestion (2). For detection, the PVDF-membrane was probed with rabbit anti-SHBG pAb, then a HRP-conjugated goat anti-rabbit IgG pAb was added; AEC was used as dye. M = molecular weight marker.

Table 1: Bioactivity of the PNGase F Digested and Gel Filtrated SHBG

sample no. ± SHBG	SHBG (nM)	free T (pM)
serum 1/− SHBG	14.7	44.1
serum 1/+ SHBG	177.4	14.4
serum 2/− SHBG	20.2	36.9
serum 2/+ SHBG	164.4	12.0
serum 3/− SHBG	28.4	47.5
serum 3/+ SHBG	180.3	17.3

documents the well-established size heterogeneity of SHBG due to variations in carbohydrate content (*34*), whereas for PNGase F digested SHBG (lane 2) the single band at 43 kDa reflects the successful deglycosylation procedure. Traces of dimeric protein were seen at 95 kDa in line 1, while no other impurities could be detected. The size-exclusion chromatography of PNGase F digested SHBG was found also to reduce endogenous steroid concentrations in the concentrated eluate from 5 to 2 nM for T, from 500 to 20 pM for E2 and from 10 to 5 nM for progesterone.

Qualitative Assessment of the Binding Activity of Purified SHBG. Three human male sera with low endogenous SHBG concentrations (approximately 20 nM) and known free T levels were spiked with the concentrated PNGase F digested and gel-filtrated SHBG solution used for the biosensor experiments, resulting in a final SHBG concentration of approximately 200 nM (mean 175 nM). The spiking of the sera produced a decrease of the free T concentrations from 42.78 ± 5.48 to 14.57 ± 2.67 pM. The data concerning the binding activity of the purified SHBG preparation are summarized in Table 1.

Kinetic Analyses Using the SPR Biosensor. Preparation of the Steroid-Coupled Biosensor Surface. SPR-based binding studies require that one of the two binding partners is immobilized on the sensor surface. In this work, the three 17α- and 1α-aminoalkyl DHT ligands (**1**−**3**) were covalently coupled to the CM dextran of the chip by use of the NHS/EDC method so as to interact with the high-molecular-weight SHBG protein, brought in solution into the flow system. This

Table 2: Kinetic and Thermodynamic Data for the DHT Derivatives **1**−**3** Derived from the SPR Biosensor Measurements[a]

compd	*n*	k_{+1} [10^{+4} M^{-1} s^{-1}]	k_{-1} [10^{-3} s^{-1}]	K_a1 [10^{+7} M^{-1}]	k_{+2} [10^{-3} RU^{-1} s^{-1}]	k_{-2} [10^{-3} s^{-1}]	K_a2 [10^{-1} RU^{-1}]
1	4	3.69 ± 0.79	25.2 ± 9.11	0.156 ± 0.044	0.05 ± 0.02	0.18 ± 0.03	3.05 ± 1.59
2	4	0.91 ± 0.24	0.55 ± 0.08	1.64 ± 0.236	11.9 ± 13.9	674 ± 160	0.15 ± 0.14
3	4	2.15 ± 0.60	0.18 ± 0.02	11.7 ± 2.12	24.7 ± 36.4	323 ± 291	0.67 ± 0.42

[a] Values are given as mean ± SD. SHBG was applied in the following concentrations: 75, 100, 175, 250 nM for **1**; 50, 100, 150, 200 nM for **2**; 75, 100, 150, 200, 400 nM for **3**. The K_a1 and K_a2 values were derived from $K_a1 = k_{+1}/k_{-1}$ and $K_a2 = k_{+2}/k_{-2}$.

Table 3: Thermodynamic Data for the DHT Derivatives **1**−**3** Derived from the Equilibrium Measurements[a]

1 (*n* = 4)			**2** (*n* = 4)			**3** (*n* = 6)			testosterone (T) (*n* = 5)
RBA (%)	*R*	K_a (10^7 M^{-1})	RBA (%)	*R*	K_a (10^7 M^{-1})	RBA (%)	*R*	K_a (10^7 M^{-1})	K_a (10^7 M^{-1})
0.62 ± 0.05	0.435 ± 0.024	1.25 ± 0.79	0.6 ± 0.01	0.395 ± 0.006	1.50 ± 0.10	52.0 ± 11.2	0.423 ± 0.041	140 ± 32	319.4 ± 31.7

[a] Ref *31*. Values are given as mean ± SD. RBA = relative binding activity; $R = B/B_0$ at 50% displacement.

design is advantageous for real time kinetic information in terms of the sensor response obtained upon binding of the macromolecular SHBG to immobilized steroidal ligands. First, the steroids are coupled covalently through a stable amide bond which prevents from loss of the ligands from the surface. Second, the relatively long 1α- and 17α-alkylamine linker arms allow an optimized recognition of the more distant of the two characteristic 3- and 17-functional groups of DHT and, possibly, at least, a partial recognition of the remaining more vicinal group. Third, a low steroidal surface density was employed to prevent major nonspecific coupling phenomena and to limit mass transfer complications.

The surface density was optimized by use of Pioneer B1-chips characterized by a low degree of carboxylation providing a lower immobilization capacity and a less negative charge, as compared with CM5 chips. The final concentration of immobilized DHT derivative, derived from the net RU increment values after coupling (100−250 RU, depending on the DHT derivative) was estimated to approximately 100−250 pg of steroid bound per mm^2.

The functionality of the steroid-coated surface for immobilizing a steroid binding protein was tested with two different anti-T mAbs (T3 and T19, both cross-reacting with DHT) which showed RU values in the range of 300−800 RU and of 200−500 RU, respectively. This is in accordance with the maximum RU values of the specific interactions measured with SHBG.

Biosensor Measurements. The CM dextran hydrogel of the FC1 cell, treated with EDC/NHS and ethanolamine in the absence of steroidal ligands, served as reference for eliminating unspecific binding. Additionally, the FC1 reference line showed that the changes due to the concentrated protein solution were low in the absence of an immobilized steroid. The resulting FC2 − FC1 difference RU values are shown as sensorgrams in Figure 3 for the interaction of SHBG with the three immobilized DHT derivatives. All data were recorded at 25 °C with four independent experiments for each tested DHT derivative. The SHBG-specific association and dissociation profiles with the DHT ligands were recorded at four different final protein concentrations ranging from 50 to 250 nM for **1** (Figure 3A), from 75 to 200 nM for **2** (Figure 3B), and from 75 to 400 nM for **3** (Figure 3C). Above the latter concentration oligomerization of SHBG occurred and limited the kinetic analysis. The figure also depicts the acceptable residuals from the fit of the SHBG interaction in the bivalent model (see below).

Kinetic Interaction Analysis. A comprehensive fitting analysis by use of the BiaEvaluation software for the interaction of SHBG with the three DHT derivatives **1**−**3** was performed. The binding and dissociation curves were fitted simultaneously for all SHBG concentrations. The fitting residuals for the sensorgrams of the interaction between SHBG and the 1α-DHT derivative **3** are exemplary presented in Figure 4. Similar residual patterns were found for the 17α-DHT compounds **1** and **2** and are presented as Supporting Information. The four possible kinetic models are (i) simple Langmuir 1:1 isotherm binding, (ii) mass transfer limited 1:1 binding, (iii) bivalent binding, and (iv) two-state reaction with conformational change. The low χ^2 residuals of the global fitting analysis (*35*) for the three ligands strongly suggested that the best fitting model is the one assuming two independent binding sites (bivalent model). All kinetic parameters are given in Table 2. These biosensor measurements further enabled the calculation of the affinity constants (K_a1) for the first step on an assumed bivalent interaction of SHBG with each of the tested DHT derivatives. The association constant K_a1 for the 1α-aminohexyl DHT derivative **3** (1.2×10^8 M^{-1}) was remarkably higher than the values observed for the 17α-aminoalkyl DHT derivatives **1** and **2** (0.16 and 1.6×10^7 M^{-1}, respectively).

Determination of Association Constants from Equilibrium Measurements. These measurements, performed by competition of the three DHT derivatives **1**−**3** with a tritiated T tracer, using the Con A-Sepharose separation technique (Table 3) have been previously reported (*31*).

Flow Cytometry Analysis Using Double Fluorescence Labeling. Flow cytometry methodologies can be easily applied to characterize proteins immobilized on silica or latex microspheres if these proteins can be labeled by capture of fluorochrome-conjugated ligand molecules. Thus, in this study, our cytometric experiments were based on the hypothesis that homodimeric SHBG could react at one of its two potential steroid-binding sites with a steroid ligand such as the 1α-DHT derivative **3**, immobilized on PE-labeled latex beads, whereas—if still active—the remaining potential binding site could also bind an additional FLUOS-labeled steroid conjugate such as the 1α-DHT derivative **4**. The detection of a double fluorescent latex bead population,

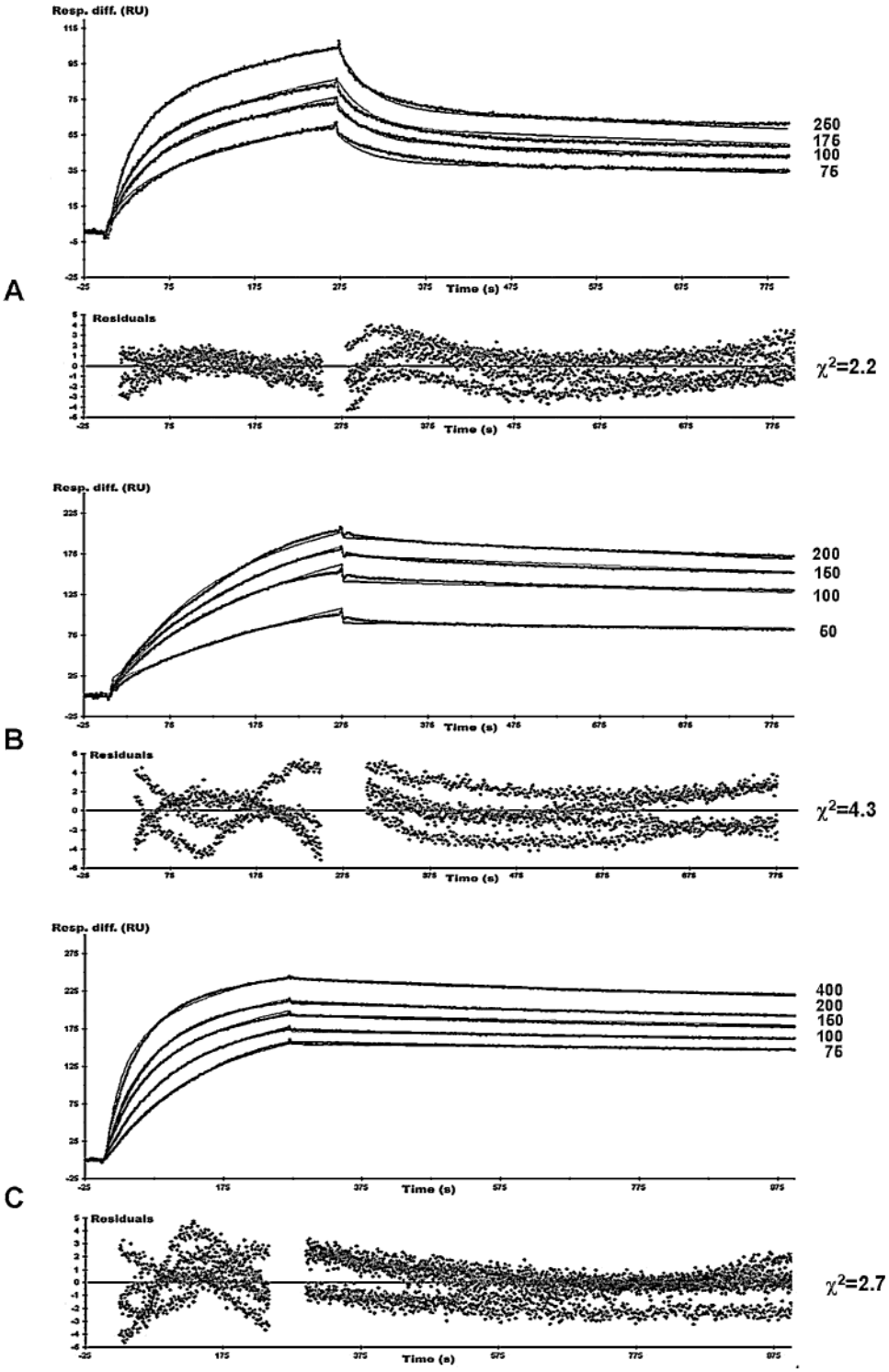

FIGURE 3: Typical sensorgram showing association and dissociation profiles of the SHBG interaction with the DHT derivatives **1** (A), **2** (B), and **3** (C) on a B1-chip surface along with the corresponding residual plots of the data fitting analysis using the bivalent analyte model.

which can only occur for SHBG still being immobilized on the beads, would support the assumption of the existence of a hybrid complex consisting of two DHT ligands bound simultaneously by each of the two monomers of homodimeric SHBG. A scheme of the experimental setup is cartooned in Figure 5.

The precision of this microsphere-based flow cytometry is contingent upon the monodispersity of the particles which could be asserted by the presence of a major population of more than 75% with low scatter properties (FSC and SSC values). A gate was set around this population and used for all flow cytometric experiments. The remaining 25% of all events were a composite of impurities and particle aggregates. Beads aggregated by cross-linking of SHBG via two immobilized 1α-DHT ligands **3** might be also present in this population. An analytical influence, however, could be prevented by the gate setting. Additionally, the latex particles were described by the manufacturer to be uniform in size with a diameter variation of 2.5%. Although this appears to be a potential analytical limitation, the ease of

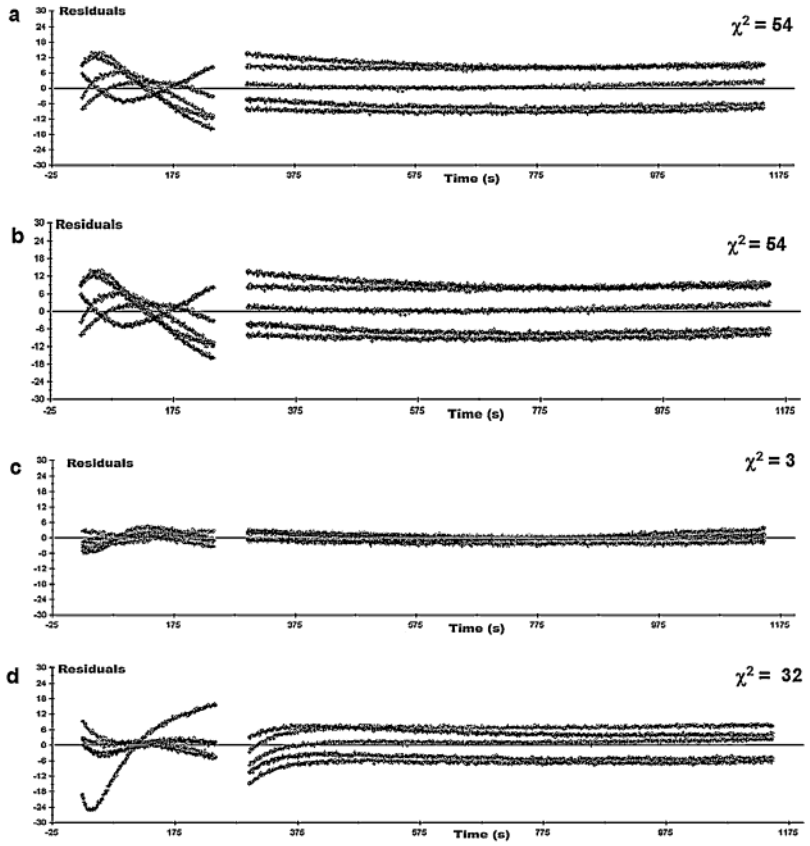

FIGURE 4: Residuals obtained by global fitting analysis of SHBG sensorgrams. Different final concentrations of SHBG (50, 75, 100, 150, 175, 200, and 400 nM) were injected over a B1 surface with 63 RU of amine-coupled 1α-DHT derivative ***3***. The kinetic models are 1:1 binding (a), 1:1 binding with mass transport limitation (b), bivalent analyte (c), and two-state reaction (d).

measuring a large number of particles (25 000 gated events) made possible a satisfying precision.

The results presented here (Figure 6) are summarized as biparametric dot plots of log FL1 values (FLUOS) vs log FL2 values (PE), representative of three independent experiments. The shift of the FLUOS/PE double positive bead fraction toward the upper right quadrant of Figure 6A indicated the formation of a SHBG hybrid complex.

A series of functional controls were performed to verify the validity of the flow cytometry results. First, a competition experiment underpined the assumption of a functional integrity of the SHBG-ligand complex: The fluorescence intensity FL1, caused by the FLUOS-labeled 1α-DHT derivative **4**, was significantly reduced by addition of a 10-fold molar excess of its unlabeled 1α-aminohexyl DHT precursor **3** (Figure 6B). This was either due to a direct displacement of **4** from SHBG or to a displacement of the latex-immobilized compound **3**, leading to a reduced amount of bound SHBG. On the other hand, a similar molar excess of the 17α-aminoalkyl DHT compound **2**, characterized by a much weaker affinity, had no inhibitory capability on the binding of compound **4** (Figure 6C) and could not significantly displace SHBG from the microspheres. Second, two control experiments were performed to check the specificity of SHBG binding. In Figure 6D, a sample, completely processed except for coupling of the steroid ligand **3** to the latex bead, is shown. The uniform bead population with low FL1 values ruled out any nonspecific binding of SHBG to the latex beads. In Figure 6E, a sample, processed without incubation with SHBG prior to the addition of the FLUOS-labeled steroid ligand **4**, proved the insignificance of nonspecific binding phenomena caused by the hydrophobic FLUOS-labeled conjugate to the bead surface. This can be derived from the mean fluorescence intensity (MFI) values of this control (MFI = 7), which is only slightly higher than that observed in Figure 6F (MFI = 3) a plot that represents latex beads being solely incubated with Biotin-PE conjugate. The MFI value for Figure 6A with both incubation with SHBG and FLUOS-labeled DHT ligand was 157. Third, the efficiency of the steroid **3**-coated latex beads to bind SHBG was proven by incubating steroid-coated latex beads with buffer alone (Figure 6G) or with SHBG (Figure 6H) and by staining in a two-step reaction with a rabbit anti-SHBG pAb and a FITC-labeled goat anti-rabbit IgG pAb.

DISCUSSION

Until recently, it was generally accepted that the homodimeric human SHBG had only a single active LBD corresponding to an equimolar relationship between the dimeric binding protein and the steroid ligand. This concept was established by numerous binding measurements with radioactive steroidal ligands including Scatchard plots at different temperatures either on serum samples or on purified SHBG (*2*). Accordingly, the hypothesis was suggested that a single LBD could be located within the dimer interface (*4*). An isolated article compared the molecular forms of SHBG in serum by HPLC and claimed that human SHBG in serum could be monomeric, whereas serum dilutions were found to induce a progressive dimerization resulting in a decrease of its apparent binding capacity (*27*). Recent crystal structure data on recombinant homodimeric LBD domains, first presented by Grishkovskaya et al. (*25*), have shown that

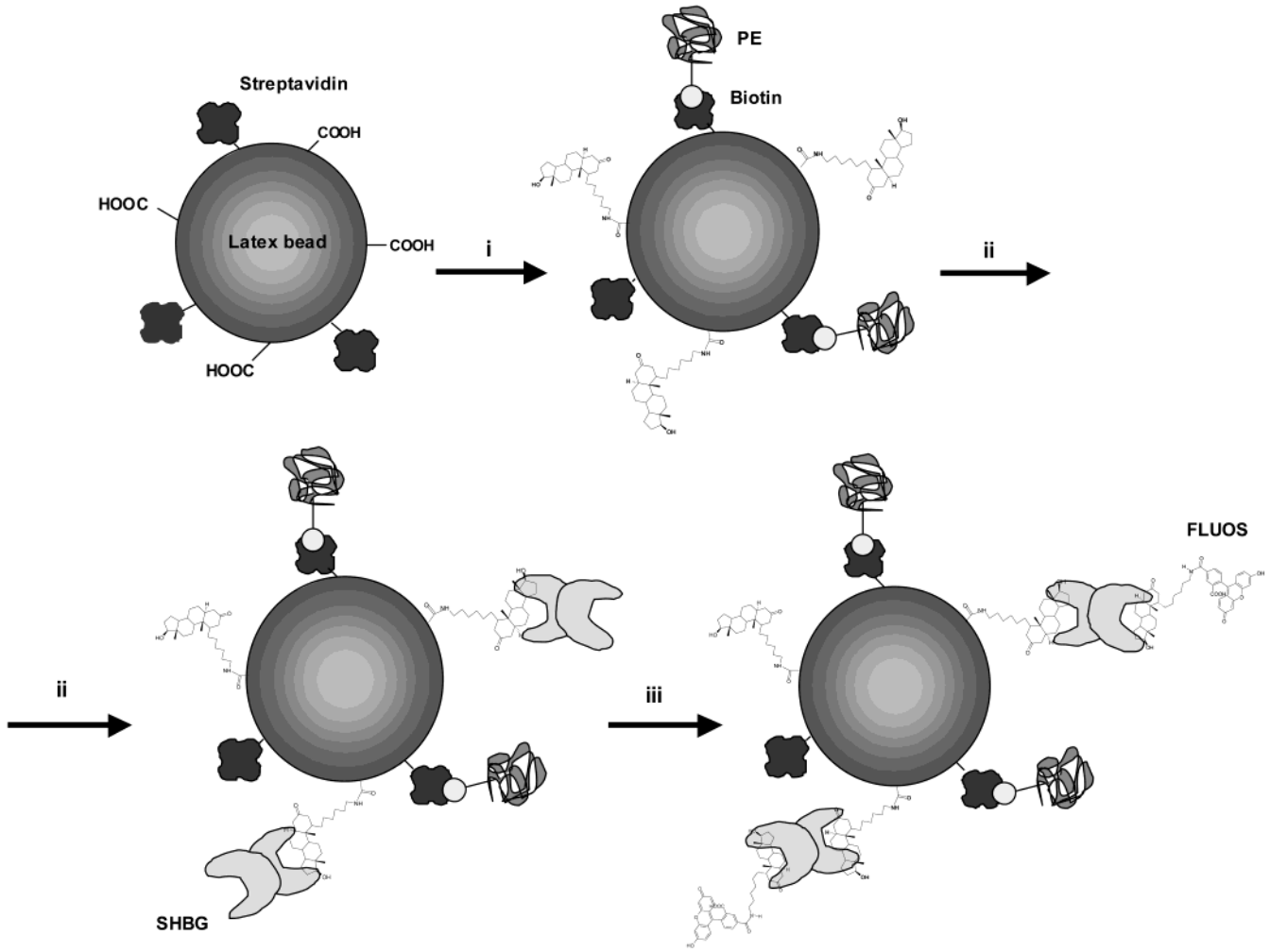

FIGURE 5: Scheme of the experimental setup to prove bivalent ligand binding of SHBG dimers by cytometric analysis using latex beads as solid support. (i) Binding of Biotin-PE to the streptavidin-linked beads and coupling of **3** via EDC/NHS-chemistry; (ii) incubation with SHBG; (iii) incubation with **4**.

each monomer contains a functional LBD for a DHT steroid molecule within the *N*-terminal laminin G-like domain. Avvakumov et al. (*26*) showed by site-directed mutagenesis that dimerization-deficient SHBG variants contain a LBD with an affinity and specificity indistinguishable from wild-type SHBG. These results raise the question whether a direct extrapolation of these findings can be made in the case of native SHBG for which the steroid-binding stoichiometry is a primordial functional parameter. In this work, steroid-binding properties of purified native SHBG were first analyzed using a biosensor methodology for which SHBG was *N*-deglycosylated to eliminate glycosylation variants which might cause a microheterogeneity leading to corrupted biosensor sensorgrams. For instance, the absence of long carbohydrate side-chains of the protein may prevent interactions with the CM dextran moieties on the chip surface which would be responsible for attenuated dissociation rates in the sensorgram.

We applied a biosensor with a photometric transducer, based on the SPR technique, as sensitive tool for the biomolecular interaction analysis. This system detects the change in mass concentration in the surface layer as a change in the RI via the SPR effect (*36*, *37*). This is an optical phenomenon producing a reduction of the intensity of a light reflected over a thin gold film at the interface between the glass support and the surface of the sensor chip. The effect is maximal at a particular angle which varies as a function of the RI according to the changes in mass concentration of the soluble protein interacting with ligands covalently attached to the flexible three-dimensional CM dextran matrix on the sensor chip of the BIAcore instrument. We used solid-state surface-bound steroid ligands and added SHBG as binding partner in solution. The DHT derivatives were modified at the 1α- and 17α-position by alkylamine spacers that can be covalently coupled to the CM dextran surface and let the opposite functional 17- or 3-groups of the steroid fully accessible for recognition according to the LBD specificity for these two complementary extremities of the DHT ligand. The great flexibility of the dextran polymer layer (*38*), which extends approximately 100 nm out of the chip surface, enables a local arrangement of two immobilized ligands in such a way that they can be sterically available for a simultaneous binding to the two end-to-end standing LBDs of the SHBG homodimer. Thus, substantial high sensor signals for mass adsorption and desorption could be obtained. Moreover, the low density of covalent attachment of the aminoalkyl DHT derivatives to B1-chips led to a stable surface, resulting in highly reproducible sensorgrams. The steroid-coated B1-chips were storable under HBS buffer at 4 °C for several months without remarkable loss of activity.

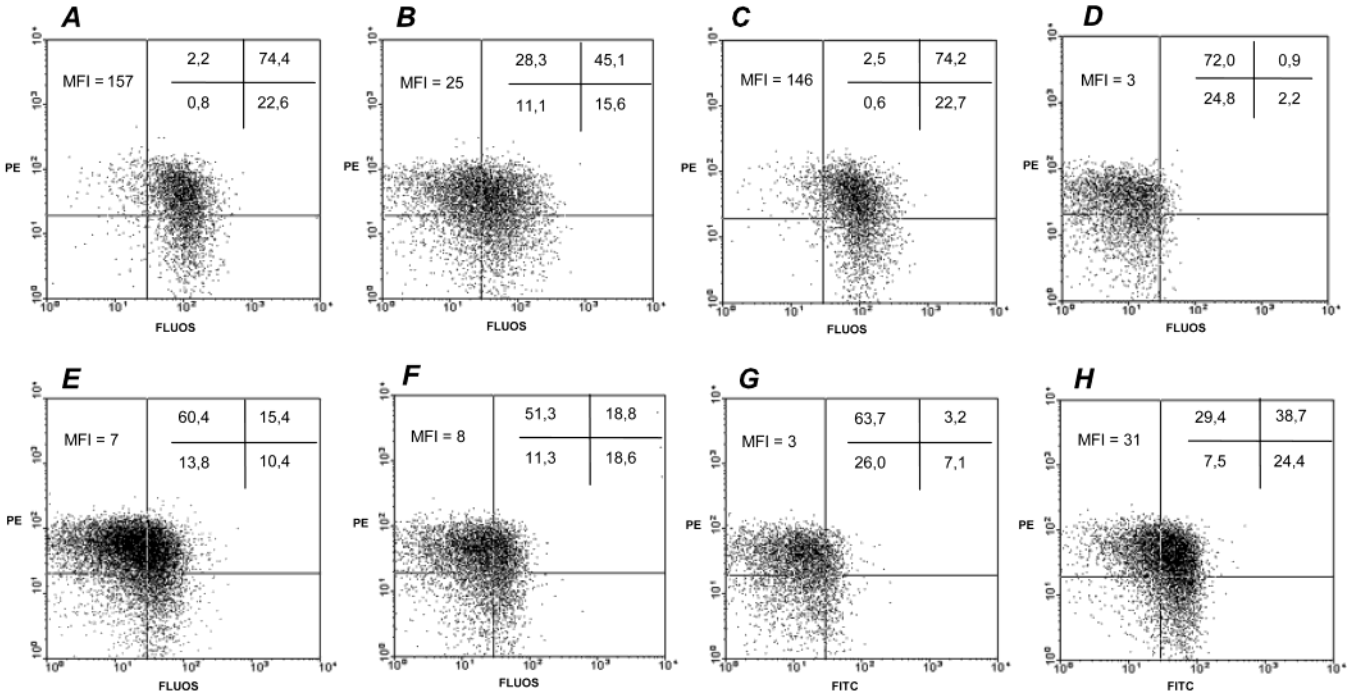

FIGURE 6: Biparametric dot plots of log FL1 (fluorescein) vs log FL2 (PE). The fluorescein/PE double positive bead fraction in (A) indicates the formation of a SHBG hybrid complex. The binding of **4** could be competed by a 10-fold molar excess of **3** (B), whereas steroid 2 has no inhibitory effect (C). In (D) the latex beads were solely incubated with biotin-PE conjugate. Samples without conjugation of **3** to the latex bead (E) or without SHBG incubation prior addition of **4** (F) served also as controls. To prove SHBG binding capability, **3**-coated beads were incubated with buffer alone (G) or SHBG (H) and subsequently stained with rabbit anti SHBG pAb and FITC-labeled goat anti rabbit IgG pAb. In the insets of each dot plot the percentages of counted events per quadrant are presented together with the MFI value of the total events for FL1.

The kinetic data from the real time molecular interaction analysis (Table 2) were evaluated by the BIAevaluation program based on numerical integration algorithms (*39*, *40*). Inherent to the method is the assumption of true association and dissociation rates for an one-to-one interaction model (*41*). The method is applied to reactions at a heterogeneous phase which have to be clearly discriminated from measurements in solution. The good fit of the experimental data with the complex bivalent analyte model is consistent with a two-step nature of the binding of the bivalent SHBG molecule with DHT derivatives immobilized at the surface (*42*). The initial intermolecular binding is defined by the affinity constant K_a1, given in M^{-1}. The affinity constant for the second binding event at the surface is K_a2, given in the unconventional unit RU^{-1}. This is because the second association rate constant k_{+2} is expressed in RU^{-1} s^{-1} as the concentration of the initial complex bound to one ligand at the surface (SHBG−DHT) is calculated during the fitting process in terms of the observed RU response. The overall affinity constant results from the sum of the free energy changes which occur in the two binding events. Thus, the association constant K_a is given by the product of the two binding constants K_a1 and K_a2 ($K_a = K_a1 \times K_a2$), its unit being M^{-1} RU^{-1}. The surface ligand capacity of the biosensor chips was calculated to be 100−200 RU for the three tested DHT derivatives as described in Results. Thus, in an approximation the K_a values for **1**−**3** must be multiplied by 150 when they are to be compared with association constants measured under equilibrium conditions (see below).

Relating to the kinetics of the interaction, it should be stated that the association rate constants for the initial SHBG−DHT complex (see Table 2) were found quite similar for all three DHT derivatives. On the other hand, the dissociation rate constants were high for **1**, in the middle range for **2** and low for **3**, explaining the stronger binding affinity of compound **3**. Then, SHBG complexed with one immobilized aminoalkyl DHT binds to another immobilized ligand to form a divalent complex. For this second step the association rate constants, but also the dissociation rate constants, are also highest for **3** with a declining tendency for **2** and **1**. The question of whether the first ligand binding event modulates the second LBD properties cannot be answered in detail solely by this investigation. However, additional circular dichroism analyses were performed (data not shown). No relevant conformational rearrangement of the end-to-end homodimeric protein could be detected.

The association constants, derived from the biosensor studies (Table 2), have to be compared with those from previously reported measurements under equilibrium conditions (Table 3) (*31*). The two unsubstituted 17α-aminoalkyl DHT derivatives **1** and **2** reacted almost identically with SHBG in the equilibrium measurements. This is comprehensible since the structural differences of both compounds are small. Functional side chains in the 17α-position, different in size and length, are well tolerated in the LBD, as described in ref *30*. The molecular size of the compounds **1** and **2** in the vicinity of the C-17 position were found quite similar according to ^{1}H NMR NOSY experiments in nonpolar solvents (*31*). One can speculate whether this observation would still be valid in aqueous medium and in the presence of the hydrophobic steroid binding site of SHBG. The K_a value of compound **2** derived from equilibrium measurements (1.50×10^7 M^{-1}) was in the same range as the K_a1 values found with the SPR biosensor analysis (1.64×10^7 M^{-1}). The K_a value of compound **1**, measured under equilibrium conditions (1.25×10^7 M^{-1}) was much higher than the K_a1

value of **1** (0.16×10^7 M^{-1}) measured with the SPR biosensor. This discrepancy, however, could be explained by sterical hindrance at the CM dextran moiety of the sensor surface due to the short linker arm of this 17α-aminoalkyl DHT derivative. The unsubstituted 1α-DHT derivative **3** showed a much higher K_a value being 140×10^7 M^{-1}, measured under equilibrium conditions, representing half of the K_a value of T (3.19×10^9 M^{-1}), measured in parallel and comparable to the K_a value of mesterolone (3.6×10^9 M^{-1}) given in the literature (*28*, *29*, *43*−*45*). The SPR technique provides for the immobilized ligand **3** a K_a1 value of 11.7×10^7 M^{-1} which represents approximately 10% of that measured under equilibrium conditions. Again a sterical hindrance at the sensor surface may be responsible for a weaker interaction of the ligand with SHBG.

Several reports raised concerns over the validity of the kinetic data generated by the SPR biosensor as they might be affected by proteic binding site heterogeneity and/or mass transfer limitations (*46*−*48*). We tried to avoid these two pitfalls by using a highly purified and functional active SHBG preparation (see Figure 2 and Table 1). Additionally a low surface density of steroid ligands bound to B1-chips (with a reduced degree of carboxylation of the CM dextran compared to CM5 chips) was applied. We could minimize variations caused by analyte heterogeneity, nonspecific binding effects or bulk RI changes. The binding interaction was not limited by mass transport in relation to the immobilization density as shown by the excellent fitting to the bivalent model and confirmed by the fact that the kinetic parameters were independent of the flow rate used (data not shown).

Flow cytometry analysis of steroid-coupled latex beads was used as a second, independent method to provide direct evidence for the presence of two functional steroid binding sites on homodimeric native SHBG. This technique can detect inert microspheres of different sizes, dyed with various fluorochromes. Microspheres have been used as calibrators and also as a solid support for numerous molecular reactions quantitated by flow cytometry. Proteins and other molecules have been adsorbed or chemically coupled to the surface of microspheres to capture analytes that are subsequently measured by a fluorochrome-conjugated detection molecule (*49*). In our study, 1α-aminohexyl DHT was covalently coupled, on one hand, to latex microspheres bearing a first fluorescence dye and, on the other hand, to a second discriminative steroid-bound fluorophore. The detection of a dual fluorescence signal directly reflected a simultaneous occupation of the two potential LBDs of native homodimeric SHBG, one by the immobilized 1α-aminohexyl DHT, and the other, by the fluorochrome-conjugated 1α-aminohexyl DHT probe molecule. Thus, the bivalent binding model, proposed for the three studied 1α- and 17α-aminoalkyl DHT by the global fitting of the SPR sensorgrams, was confirmed by this analytical technique at least for the 1α-aminohexyl DHT derivative **3**, reflecting the ligand-binding situation in solution without any interferences by a solid-state surface. Flow cytometry measurements with the 17α-aminoalkyl DHT analogues **1** and **2** under similar experimental conditions could not be performed due to the lower binding affinities of these ligands to SHBG.

In summary, the SPR biosensor as well as flow cytometry analyses of this study revealed for the first time a bivalent interaction of native human SHBG with a novel 1α-aminohexyl DHT ligand structure, fully consistent with the presence of two active binding sites, recently suggested by X-ray crystallography of recombinant human homodimeric SHBG fragments of Grishkovskaya et al. (*25*) and by binding studies of nondimerizable SHBG mutant monomers, performed by Avvakumov et al. (*26*). It remains to be verified whether this conclusion depends on binding properties specific of immobilized 1α-aminohexyl DHT derivatives or can be extended to other steroid ligands of lower affinity such as 17α-aminoalkyl DHT. Although the bivalent binding characteristics of these 17α-derivatives were also strongly suggested by the SPR biosensor kinetic studies, this still needs to be confirmed by a second technique. The flow cytometry technique, however, could not be extended to these ligands of lower binding affinity. Our study may be relevant for a better understanding of SHBG-ligand interactions with natural and synthetic steroids as well as environmental nonsteroidal ligands and therefore of the role of SHBG in endocrinopathies with underlying hyperandrogenic disease states with impaired SHBG metabolism and possibly altered biological function.

ACKNOWLEDGMENT

We thank Prof. Arne Skerra, Weihenstephan, and Dr. Hans-Joachim Gross, Erlabrunn, for fruitful discussions.

SUPPORTING INFORMATION AVAILABLE

A complete set of tables and figures concerning the biosensor measurements for the three DHT derivatives. This material is available free of charge via the Internet at http://pubs.acs.org.

REFERENCES

1. Anderson, D. C. (1974) Sex-hormone-binding globulin. *Clin. Endocrinol. (Oxf.) 3*, 69−96.
2. Hammond, G. L. (1990) Molecular properties of corticosteroid binding globulin and the sex-steroid binding proteins. *Endocr. Rev. 11*, 65−79.
3. Westphal, U. (1986) Steroid-protein interactions II. *Monogr. Endocrinol. 27*, 198−264.
4. Petra, P. H. (1991) The plasma sex steroid binding protein (SBP or SHBG). A critical review of recent developments on the structure, molecular biology and function. *J. Steroid Biochem. Mol. Biol. 40*, 735−753.
5. Joseph, D. R. (1994) Structure, function, and regulation of androgen-binding protein/sex hormone-binding globulin. *Vitam. Horm. 49*, 197−280.
6. Hammond, G. L., Underhill, D. A., Rykse, H. M., and Smith, C. L. (1989) The human sex hormone-binding globulin gene contains exons for androgen-binding protein and two other testicular messenger RNAs. *Mol. Endocrinol. 3*, 1869−1876.
7. Berubé, D., Seralini, G. E., Gagne, R., and Hammond, G. L. (1990) Localization of the human sex hormone-binding globulin gene (SHBG) to the short arm of chromosome 17 (17p12 → p13). *Cytogenet. Cell Genet. 54*, 65−67.
8. Walsh, K. A., Titani, K., Takio, K., Kumar, S., Hayes, R., and Petra, P. H. (1986) Amino acid sequence of the sex steroid binding protein of human blood plasma. *Biochemistry 25*, 7584−7590.
9. Hammond, G. L., Underhill, D. A., Smith, C. L., Goping, I. S., Harley, M. J., Musto, N. A., Cheng, C. Y., and Bardin, C. W. (1987) The cDNA-deduced primary structure of human sex hormone-binding globulin and location of its steroid-binding domain. *FEBS Lett. 215*, 100−104.
10. Strel'chyonok, O. A., and Avvakumov, G. V. (1990) Specific steroid-binding glycoproteins of human blood plasma: novel data on their structure and function. *J. Steroid Biochem. 35*, 519−534.
11. Hildebrand, C., Bocchinfuso, W. P., Dales, D., and Hammond, G. L. (1995) Resolution of the steroid-binding and dimerization domains of human sex hormone-binding globulin by expression in *Escherichia coli*. *Biochemistry 34*, 3231−3238.

12. Bocchinfuso, W. P., and Hammond, G. L. (1994) Steroid-binding and dimerization domains of human sex hormone-binding globulin partially overlap: steroids and Ca^{2+} stabilize dimer formation. *Biochemistry 33*, 10622−10629.
13. Bardin, C. W., and Lipsett, M. B. (1967) Testosterone and androstenedione blood production rates in normal women and women with idiopathic hirsutism or polycystic ovaries. *J. Clin. Invest. 46*, 891−902.
14. Vermeulen, A. L., Verdonck, L., Van der Straeten, M., and Orie, M. (1969) Capacity of the testosterone binding globulin in human plasma and influence of specific binding of testosterone on its metabolic clearance rate. *J. Clin. Endocrinol. Metab. 29*, 1470−1480.
15. Petra, P. H., Stanczyk, F. Z., Namkung, P. C., Fritz, M. A., and Novy, M. J. (1985) Direct effect of sex steroid-binding protein (SBP) of plasma on the metabolic clearance rate of testosterone in the rhesus macaque. *J. Steroid Biochem. 22*, 739−746.
16. Plymate, S. R., Namkung, P. C., Metej, L. A., and Petra, P. H. (1990) Direct effect of plasma sex hormone binding globulin (SHBG) on the metabolic clearance rate of 17β-estradiol in the primate. *J. Steroid Biochem. 36*, 311−317.
17. Bordin, S., and Petra, P. H. (1980) Immunocytochemical localization of the sex steroid-binding protein of plasma in tissues of the adult monkey *Macaca nemestrina*. *Proc. Natl. Acad. Sci. U.S.A. 77*, 5678−5682.
18. Strel'chyonok, O. A., Avvakumov, G. V., and Survilo, L. I. (1984) A recognition system for sex-hormone-binding protein-estradiol complex in human decidual endometrium plasma membranes. *Biochim. Biophys. Acta 802*, 459−66.
19. Pardridge, W. M. (1988) Selective delivery of sex steroid hormones to tissues in vivo by albumin and by sex hormone-binding globulin. *Ann. N. Y. Acad. Sci. 538*, 173−192.
20. Nakhla, A. M., Khan, M. S., and Rosner, W. (1990) Biologically active steroids activate receptor-bound human sex hormone-binding globulin to cause LNCaP cells to accumulate adenosine 3′,5′-monophosphate. *J. Clin. Endocrinol. Metab. 71*, 398−404.
21. Fissore, F., Fortunati, N., Comba, A., Fazzari, A., Gaidano, G., Berta, L., and Frairia, R. (1994) The receptor-mediated action of sex steroid binding protein (SBP, SHBG): accumulation of cAMP in MCF-7 cells under SBP and estradiol treatment. *Steroids 59*, 661−667.
22. Lim, S. C., Caballero, A. E., Arora, S., Smakowski, P., Bashoff, E. M., Brown, F. M., Logerfo, F. W., Horton, E. S., and Veves, A. (1999) The effect of hormonal replacement therapy on the vascular reactivity and endothelial function of healthy individuals and individuals with type 2 diabetes. *J. Clin. Endocrinol. Metab. 84*, 4159−4164.
23. Carlström, K., Gershagen, S., and Rannevik, G. (1987) Free testosterone and testosterone/SHBG index in hirsute women: a comparison of diagnostic accuracy. *Gynecol. Obstet. Invest. 24*, 256−261.
24. Hammond, G. L., and Bocchinfuso, W. P. (1995) Sex hormone-binding globulin/androgen-binding protein: steroid-binding and dimerization domains. *J. Steroid Biochem. Mol. Biol. 53*, 543−552.
25. Grishkovskaya, I., Avvakumov, G. V., Sklenar, G., Dales, D., Hammond, G. L., and Muller, Y. A. (2000) Crystal structure of human sex hormone-binding globulin: steroid transport by a laminin G-like domain. *EMBO J. 19*, 504−512.
26. Avvakumov, G. V., Grishkovskaya, I., Muller, Y. A., and Hammond, G. L. (2001) Resolution of the human sex hormone-binding globulin dimer interface and evidence for two steroid-binding sites per homodimer. *J. Biol. Chem. 276*, 34453−34457.
27. Englebienne, P., Van Hoorde, P., and Verheyden, R. (1987) Dimerization of SHBG by gelatin and dithiothreitol. Implications for the measurement of SHBG binding capacity in human serum. *J. Steroid Biochem. 26*, 527−534.
28. Dunn, J. F., Nisula, B. C., and Rodbard, D. (1981) Transport of steroid hormones: binding of 21 endogenous steroids to both testosterone-binding globulin and corticosteroid-binding globulin in human plasma. *J. Clin. Endocrinol. Metab. 53*, 58−68.
29. Pugeat, M. M., Dunn, J. F., and Nisula, B. C. (1981) Transport of steroid hormones: interaction of 70 drugs with testosterone-binding globulin and corticosteroid-binding globulin in human plasma. *J. Clin. Endocrinol. Metab. 53*, 69−75.
30. Grishkovskaya, I., Avvakumov, G. V., Hammond, G. L., Catalano, M. G., and Muller, Y. A. (2002) Steroid ligands bind human sex hormone-binding globulin in specific orientations and produce distinct changes in protein conformation. *J. Biol. Chem. 277*, 32086−32093.
31. Hauptmann, H., Metzger, J., Schnitzbauer, A., Cuilleron, C. Y., Mappus, E., and Luppa, P. B. (2003) Syntheses and ligand-binding studies of 1α- and 17α-aminoalkyl dihydrotestosterone derivatives to human sex hormone-binding globulin. *Steroids 68*, 629−639.
32. Adamczyk, M., Chen, Y. Y., Gebler, J. C., Johnson, D. D., Mattingly, P. G., Moore, J. A., Reddy, R. E., Wu, J., and Yu, Z. (2000) Evaluation of chemiluminescent estradiol conjugates by using a surface plasmon resonance detector. *Steroids 65*, 295−303.
33. Lutz, R. A., Märki, H. H., and Weder, H. G. (1977) Die Androgenbindung im menschlichen Plasma und ihre physiologische Bedeutung. *J. Clin. Chem. Clin. Biochem. 15*, 57−67.
34. Danzo, B. J., Bell, B. W., and Black, J. H. (1989) Human testosterone-binding globulin is a dimer composed of two identical protomers that are differentially glycosylated. *Endocrinology 124*, 2809−2817.
35. De Crescenzo, G., Grothe, S., Zwaagstra, J., Tsang, M., and O'Connor-McCourt, M. D. (2001) Real-time monitoring of the interactions of transforming growth factor-beta (TGF-beta) isoforms with latency-associated protein and the ectodomains of the TGF-beta type II and III receptors reveals different kinetic models and stoichiometries of binding. *J. Biol. Chem. 276*, 29632−29643.
36. Jönsson, U., and Malmqvist, M. (1992) Real time biospecific interaction analysis, the integration of surface plasmon resonance detection, general biospecific interface chemistry and microfluidics into one analytical system. *Adv. Biosens. 2*, 291−336.
37. Van Regenmortel, M. H., Altschuh, D., Chatellier, J., Christensen, L., Rauffer-Brùyere, N., Richalet-Secordel, P., Witz, J., and Zeder-Lutz, G. (1998) Measurement of antigen−antibody interactions with biosensors. *J. Mol. Recognit. 11*, 163−167.
38. Löfås, S., and Johnsson, B. (1990) A novel hydrogel matrix on gold surfaces in surface plasmon resonance sensors for fast and efficient covalent immobilization of ligands. *J. Chem. Soc. Chem. Commun. 21*, 1526−1528.
39. Karlsson, R., Michaelsson, A., and Mattsson, L. (1991) Kinetic analysis of monoclonal antibody−antigen interactions with a new biosensor based analytical system. *J. Immunol. Methods 145*, 229−240.
40. Fagerstam, L. G., Frostell, A., Karlsson, R., Kullman, M., Larsson, A., Malmqvist, M., and Butt, H. (1990) Detection of antigen−antibody interactions by surface plasmon resonance. Application to epitope mapping. *J. Mol. Recognit. 3*, 208−214.
41. Nieba, L., Krebber, A., and Plückthun, A. (1996) Competition BIAcore for measuring true affinities: Large differences from values determined from binding kinetics. *Anal. Biochem. 234*, 155−165.
42. Cooper, M. A., and Williams, D. H. (1999) Kinetic analysis of antibody−antigen interactions at a supported lipid monolayer. *Anal. Biochem. 276*, 36−47.
43. Grenot, C., Montard de, A., Blachère, T., Ravel de, M. R., Mappus, E., and Cuilleron, C. Y. (1992) Characterization of Met-139 as the photolabeled amino acid residue in the steroid binding site of sex hormone binding globulin using D6 derivates of either testosterone or estradiol as unsubstituted photoaffinity labeling reagents. *Biochemistry 31*, 7609−7621.
44. Martin, M. E., Haourigui, M., Pelissero, C., Benassayag, C., and Nunez, E. A. (1996) Interactions between phytoestrogens and human sex steroid binding protein. *Life Sci. 58*, 429−436.
45. Vigersky, R. A., Kono, S., Sauer, M., Lipsett, M. B., and Loriaux, D. L. (1979) Relative binding of testosterone and estradiol to testosterone-estradiol-binding globulin. *J. Clin. Endocrinol. Metab. 49*, 899−904.
46. Fong, C. C., Lai, W. P., Leung, Y. C., Lo, S. C., Wong, M. S., and Yang, M. (2002) Study of substrate-enzyme interaction between immobilized pyridoxamine and recombinant porcine pyridoxal kinase using surface plasmon resonance biosensor. *Biochim. Biophys. Acta 1596*, 95−107.
47. Myszka, D. G. (1997) Kinetic analysis of macromolecular interactions using surface plasmon resonance biosensors. *Curr. Opin. Biotechnol. 8*, 50−57.
48. Schuck, P. (1996) Kinetics of ligand binding to receptor immobilized in a polymer matrix, as detected with an evanescent wave biosensor. I. A computer simulation of the influence of mass transport. *Biophys. J. 70*, 1230−1249.
49. Kellar, K. L., and Iannone, M. A. (2002) Multiplexed microsphere-based flow cytometric assays. *Exp. Hematol. 30*, 1227−1237.

BI035269K